Inorg. Chem. **2004**, *43*, 7369–7379

Influence of Anionic Functions on the Coordination and Photophysical Properties of Lanthanide(III) Complexes with Tridentate Bipyridines

Steve Comby,[†] Daniel Imbert,[†] Anne-Sophie Chauvin,[†] Jean-Claude G. Bünzli,*[,†] Loïc J. Charbonnière,[‡] and Raymond F. Ziessel*[,‡]

Laboratory of Lanthanide Supramolecular Chemistry, Swiss Federal Institute of Technology, BCH 1402, CH-1015 Lausanne, Switzerland, and Laboratoire de Chimie Moléculaire, UMR 7008 au CNRS, ECPM, 25 rue Becquerel, 67087 Strasbourg Cedex 02, France

Received July 6, 2004

A series of four ligands based on a 5′-methyl-2,2′-bipyridyl framework substituted in the 6 position by a carboxylic acid, a phosphonic acid, a monoethyl ester phosphonic acid, or a diethyl ester phosphonic acid are described. The pK_a values of all ligands and their assignments are determined by a combination of UV–vis absorption spectroscopy and ^{1}H and ^{31}P NMR spectroscopy. The ability of the tridentate ligands to form complexes with trivalent lanthanide cations (Ln = La, Nd, Eu, and Lu) in buffered water solutions (Tris-HCl, pH = 7.4) is studied by UV–vis absorption spectroscopy and ^{1}H NMR. While the two ester ligands display a weak coordination ability toward lanthanide cations, the acid ligands form stable complexes with 1:1, 1:2, and 1:3 Ln/L ratios. A weak selectivity is observed for the middle of the lanthanide series, and the complexes of the phosphonic acid derivative are up to 2 orders of magnitude more stable than those of the carboxylic acid ligand. Photophysical properties of the free phosphonic and carboxylic acid ligands and of their complexes with La, Eu, Gd, Tb, and Lu are investigated in buffered aqueous solutions both at room temperature and 77 K. An efficient ligand-to-metal energy transfer is observed for both the Eu and Tb complexes. Despite a relatively large energy gap between the ligand-centered $^3\pi\pi^*$ and the Eu($^5D_0$) or Tb($^5D_4$) emitting states, the metal-centered luminescence is well sensitized with quantum yields reaching up to 45.5 and 42.2% for the Tb 1:3 complexes with carboxylic and phosphonic acid ligands, respectively.

Introduction

The weak steric preferences of lanthanide cations make the control of their inner coordination sphere a remarkable challenging field of research, particularly if one wants to take advantage of the exceptional physicochemical properties of this series of elements. While most of the early industrial applications of lanthanide elements dealt with inorganic salts and oxides, coordination compounds have now gained major importance in fields of NMR imaging with gadolinium complexes,[1] NMR shift reagents and lanthanide-induced shift (LIS) analysis,[2] luminescent probes,[3] and time-resolved fluoroimmunoassays.[4] More recently the development of organic light-emitting diodes[5] and dopants for fiber amplifiers and lasers[6] has added to this interest.

Luminescent lanthanide ions are well suited for the design of stains for biomedical analysis, in view of their long luminescence lifetimes (in the millisecond range for several ions), large Stokes' shift, and very narrow emission bands spanning from the visible to the near-infrared. Yet, good

* Authors to whom correspondence should be addressed. E-mail: jean-claude.bunzli@epfl.ch (J.-C.G.B.), ziessel@chimie.u-strasbg.fr (R.F.Z.). Phone: (+41) 21 693 98 21 (J.-C.G.B.), (+33) 03 90 24 26 89 (R.F.Z.). Fax: (+41) 21 693 98 25 (J.-C.G.B.), (+33) 03 90 24 26 89 (R.F.Z.).

[†] Swiss Federal Institute of Technology.

[‡] UMR 7008 au CNRS.

(1) (a) Merbach, A. M.; Toth-Jakab, E. In *The Chemistry of Contrast Agents in Medical Magnetic Resonance Imaging*; Wiley: London, 2001. (b) Caravan, P.; Ellison, J. E.; McMurry, T. J.; Lauffer, R. D. *Chem. Rev.* **2002**, *102*, 2293. (c) Woods, M.; Kovacs, Z.; Sherry, A. D. *J. Supramol. Chem.* **2002**, *2*, 1. (d) Aime, S.; Cabella, C.; Colombatto, S.; Crich, S. G.; Gianolio, E.; Maggioni, F. J. *Magn. Reson. Imaging* **2002**, *16*, 394.

(2) Piguet, C.; Geraldes, C. F. G. C. In *Handbook on the Physics and Chemistry of Rare Earths*; Geschneidner, K. A., Jr.; Pecharsky, V., Bünzli, J.-C. G., Eds.; Elsevier Science BV: Amsterdam, 2003; Vol. 33, Chapter 215.

(3) (a) Bünzli, J.-C. G. In *Metal Complexes in Tumor Diagnosis and as Anticancer Agents*; Sigel, A., Sigel, H., Eds.; Metal Ions in Biological Systems, Vol. 42; Marcel Dekker Inc.: New York, 2004; Chapter 2. (b) Bünzli, J.-C. G. In *Rare Earth Luminescent Centers in Organic and Biochemical Compounds*; Liu, G. K. M., Jacquier, B., Eds.; Springer-Verlag: Berlin, 2004; Chapter 11. (c) Bünzli, J.-C. G. In *Lanthanide Probes in Life, Chemical and Earth Sciences. Theory and Practice*; Bünzli, J.-C. G., Choppin, G. R., Eds.; Elsevier Science BV: Amsterdam, 1989; Chapter 7.

10.1021/ic049118x CCC: $27.50
Published on Web 10/20/2004

luminescence properties require an efficient shielding of the cation from detrimental radiationless deactivations occurring upon interaction with OH, NH, and CH oscillators of the solvent molecules.[7] In their trivalent form, the most stable for lanthanide cations in aqueous solutions, coordination numbers of 8 or 9 are prevailing and the simplest way to fill entirely the first coordination sphere is to use four bidentate[8] or three tridentate ligands. The latter case is probably the most studied and makes use of symmetrical tridentate ligands such as pyridine-2,6-dicarboxylate,[9] terpyridines,[10] bis(benzimidazolepyridines),[11] and numerous extensions on C_3-symmetric podands.[12] Numerous macrocyclic complexes[13] as well as dinuclear[14] and trinuclear[15] triple helicates have also been reported. Saturation of the first coordination sphere is not a sufficient condition for obtaining luminescent lanthanide complexes: high thermodynamic stability and kinetic inertness in solution are also required to avoid decomplexation. Introduction of anionic charges such as carboxylate or phosphonate functions on the organic core brings stabilization through electrostatic interactions with the trivalent cations. In addition, the very weak oscillator strengths of f−f electronic transitions centered on lanthanide elements often preclude their direct excitations unless powerful sources such as lasers are used. Indirect excitation is then achieved by the so-called "antenna effect",[16] which consists of bringing in close proximity to the lanthanide a chromophoric unit that absorbs light and relays the photonic energy to the cation. The crucial choice of adequate chromophores is mainly guided by the lanthanide-centered emitting level and must take into account the possibility of energy losses due to back energy transfer[3,17] or ligand-to-metal charge transfer (LMCT) states.[3,18] The bidentate 2,2′-bipyridine (bipy) ligand is known to be a ligand of choice for generating antenna effect with lanthanide complexes.[13b,19−21] Unfortunately, the diimine moiety is not hard enough to ensure high stability in polar solvents, thereby restricting its use to organic solvents. Previous work[21a,22] showed that the introduction of two anionic carboxylate functions in 6 and 6′ positions of a bipy leads to tetradentate ligands able to form water-stable complexes with ML and ML_2 stoichiometries that display promising photophysical properties.[23] Introduction of a single carboxylic group in the 6 position of the bipy was the next trial toward the design of tridentate water-soluble chromophoric ligands. Prior work in this field[24,25] has shown that such ligands can be engineered by

(4) (a) Hemmilä, I.; Mukkala, V. *Crit. Rev. Clin. Lab. Sci.* **2001**, *38*, 441. (b) *Bioanalytical Applications of Labeling Technologies*; Hemmilä, I., Ståhlberg, T., Mottram, P., Eds.; Wallac Oy: Turku, Finland, 1995. (c) Yam, V. W.-W.; Lo, K. K.-W. *Coord. Chem. Rev.* **1998**, *184*, 157.

(5) Kido, J.; Okamoto, Y. *Chem. Rev.* **2002**, *102*, 2357.

(6) Kuriki, K.; Koike, Y.; Okamoto, Y. *Chem. Rev.* **2002**, *102*, 2347.

(7) (a) Horrocks, W. DeW., Jr.; Sudnick, D. R. *J. Am. Chem. Soc*. **1979**, *101*, 334. (b) Horrocks, W. DeW., Jr.; Sudnick, D. R. *Acc. Chem. Res.* **1981**, *14*, 384. (c) Supkowski, R. M.; Horrocks, W. DeW., Jr. *Inorg. Chim. Acta* **2002**, *340*, 44. (d) Yanagida, S.; Hasegawa, Y.; Murakoshi, K.; Wada, Y.; Nakashima, N.; Yamanaka, T. *Coord. Chem. Rev*. **1998**, *171*, 461. (e) Beeby, A.; Clarkson, I. M.; Dickins, R. S.; Faulkner, S.; Parker, D.; Royle, L.; de Sousa, A. S.; Williams, J. A. G.; Woods, M. *J. Chem. Soc., Perkin Trans. 2* **1999**, 493.

(8) (a) Binnemans, K.; Lenarts, P.; Driesen, K.; Görller-Walrand, C. *J. Mater. Chem.* **2004**, *14*, 191. (b) Shavaleev, N. M.; Pope, S. J. A.; Bell, Z. R.; Faulkner, S.; Ward, M. D. *J. Chem. Soc., Dalton Trans.* **2003**, 808. (c) de Mello Donegá, C.; Junior, S. A.; de Sá, G. F. *Chem. Commun.* **1996**, 1199. (d) de Sá, G. F.; Malta, O. L.; de Mello Donegá, C.; Simas, A. M.; Longo, R. L.; anta-Cruz, P. A.; da Silva, E. F., Jr. *Coord. Chem. Rev.* **2000**, *196*, 165.

(9) (a) Brayshaw, P. A.; Bünzli, J.-C. G.; Froidevaux, P.; Harrowfield, J. M.; Kim, Y.; Sobolev, A. N. *Inorg. Chem.* **1995**, *34*, 2068. (b) Harrowfield, J. M.; Kim, Y.; Skelton, B. W.; White, A. H. *Aust. J. Chem.* **1995**, *48*, 807.

(10) (a) Chapman, R. D.; Loda, R. T.; Riehl, J. P.; Schwartz, R. W. *Inorg. Chem.* **1984**, *23*, 1652. (b) Durham, D. A.; Frost, G. H.; Hart, F. A. *J. Inorg. Nucl. Chem.* **1969**, *31*, 833.

(11) (a) Renaud, F.; Piguet, C.; Bernardinelli, G.; Bünzli, J.-C. G.; Hopfgartner, G. *Chem. Eur. J.* **1997**, *3*, 1646. (b) Petoud, S.; Bünzli, J.-C. G.; Renaud, F.; Piguet, C.; Schenk, K. J.; Hopfgartner, G. *Inorg. Chem.* **1997**, *36*, 5750. (c) Yang, C.; Chen, X.-M.; Zhang, W. H.; Chen, J.; Yang, Y.-S.; Gong, M.-L. *J. Chem. Soc., Dalton Trans.* **1996**, 1767. (d) Platas-Iglesias, C.; Piguet, C.; André, N.; Bünzli, J.-C. G. *J. Chem. Soc., Dalton Trans.* **2001**, 3084. (e) Petoud, S.; Bünzli, J.-C. G.; Schenk, K.; Piguet, C. *Inorg. Chem.* **1997**, *36*, 1345. (f) Mallet, C.; Thummel R. P.; Hery, C. *Inorg. Chim. Acta* **1993**, *210*, 223. (g) Renaud, F.; Piguet, C.; Bernardinelli, G.; Bünzli, J.-C. G.; Hopfgartner, G. *Chem. Eur. J.* **1997**, *3*, 1660.

(12) (a) Bretonnière, Y.; Wietzke, R.; Lebrun, C.; Mazzanti, M.; Pécaut, J. *Inorg. Chem.* **2000**, *39*, 3499. (b) Senegas, J.-M.; Bernardinelli, G.; Imbert, D.; Bünzli, J.-C. G.; Morgantini, P.-Y.; Weber, J.; Piguet, C. *Inorg. Chem.* **2003**, *42*, 4680. (c) Koeller, S.; Bernardinelli, G.; Bocquet, B.; Piguet, C. *Chem. Eur. J.* **2003**, *9*, 1062. (d) Koeller, S.; Bernardinelli, G.; Piguet, C. *J. Chem. Soc., Dalton Trans.* **2003**, 2395. (e) Renaud, F.; Piguet, C.; Bernardinelli, G.; Bünzli, J.-C. G.; Hopfgartner, G. *J. Am. Chem. Soc.* **1999**, *121*, 9326.

(13) (a) Charbonnière, L. J.; Ziessel, R.; Guardigli, M.; Roda, A.; Sabbatini, N.; Césario, M. *J. Am. Chem. Soc.* **2001**, *123*, 2436. (b) Prodi, L.; Maestri, M.; Ziessel, R.; Balzani, V. *Inorg. Chem.* **1991**, *30*, 3798. (c) Bodar-Houillon, F.; Marsura, A. *New J. Chem.* **1996**, *20*, 1041. (d) Tei, L.; Baum, G.; Blake, A. J.; Fenske, D.; Schröder, M. *J. Chem. Soc., Dalton Trans.* **2000**, 2793.

(14) (a) Elhabiri, M.; Scopelliti, R.; Bünzli, J.-C. G.; Piguet, C. *J. Am. Chem. Soc.* **1999**, *121*, 10747. (b) Lessmann, J. L.; Horrocks, W. DeW., Jr. *Inorg. Chem.* **2000**, *39*, 3114. (c) Imbert, D.; Cantuel, M.; Bünzli, J.-C. G.; Bernardinelli, Piguet, C. *J. Am. Chem. Soc.* **2003**, *125*, 15698 and references therein.

(15) Floquet, S.; Ouali, N.; Bocquet, B.; Bernardinelli, G.; Imbert, D.; Bünzli, J.-C. G.; Hopfgartner, G.; Piguet, C. *Chem. Eur. J.* **2003**, *9*, 1860.

(16) (a) Sabbatini, N.; Guardigli, M.; Lehn, J.-M. *Coord. Chem. Rev.* **1993**, *123*, 201. (b) Weissmann, S. I. *J. Chem. Phys.* **1942**, *10*, 214.

(17) Charbonnière, L. J.; Balsiger, C.; Schenk, K. J.; Bünzli, J.-C. G. *J. Chem. Soc., Dalton Trans.* **1998**, 505.

(18) (a) Bünzli, J.-C. G.; Froidevaux, P.; Harrowfield, J. M. *Inorg. Chem.* **1993**, *32*, 3306. (b) Gonçalves e Silva, F. R.; Longo, R. L.; Malta, O. L.; Piguet, C.; Bünzli, J.-C. G., *Phys. Chem. Chem. Phys.* **2000**, *2*, 5400.

(19) (a) Ulrich, G.; Ziessel, R.; Manet, I.; Guardigli, M.; Sabbatini, N.; Fraternali, F.; Wipff, G., *Chem. Eur. J.* **1997**, *3*, 1815. (b) Ulrich, G.; Hissler, M.; Ziessel, R.; Manet, I.; Sarti, G.; Sabbatini, N. *New J. Chem.* **1997**, *21*, 147.

(20) (a) Alpha, B.; Lehn, J.-M.; Mathis, G. *Angew. Chem., Int. Ed. Engl.* **1987**, *26*, 266. (b) Alpha, B.; Balzani, V.; Lehn, J.-M.; Perathoner, S.; Sabbatini, N. *Photochem. Photobiol.* **1990**, *52*, 299. (c) Bazzicalupi, C.; Bencini, A.; Bianchi, A.; Giorgi, C.; Fusi, V.; Masotti, A.; Valtancoli, B.; Roque, A.; Pina, F. *Chem. Commun.* **2000**, 561.

(21) (a) Mukkala, V.-M.; Kwiatkowski, M.; Kankare, J.; Takalo, H. *Helv. Chim. Acta* **1993**, *76*, 893. (b) Mukkala, V.-M.; Kankare, J. *Helv. Chim. Acta* **1992**, *75*, 1578. (c) Couchet, J.-M.; Galaup, C.; Tisnès, P.; Picard, C. *Tetrahedron Lett.* **2003**, *44*, 4869. (d) Fisher, C.; Sarti, G.; Casnati, A.; Carretoni, B.; Manet, I.; Schuurman, R.; Guardigli, M.; Sabbatini, N.; Ungaro, R. *Chem. Eur. J.* **2000**, *6*, 1026. (e) Døssing, A.; Toflund, H.; Hazell, A.; Bourassa, J.; Ford, P. C. *J. Chem. Soc., Dalton Trans.* **1997**, 335.

(22) Sammes, P. G.; Shek, L.; Watmore, D. *Chem. Commun.* **2000**, 1625.

(23) Bünzli, J.-C. G.; Charbonnière, L. J.; Ziessel, R. F. *J. Chem. Soc., Dalton Trans.* **2000**, 1917.

(24) (a) Charbonnière, L. J.; Weibel, N.; Ziessel, R. *J. Org. Chem.* **2002**, *67*, 3933. (b) Charbonnière, L. J.; Weibel, N.; Ziessel, R. *Tetrahedron Lett.* **2001**, *42*, 659. (c) Charbonnière, L. J.; Weibel, N.; Ziessel, R. *Synthesis* **2002**, *8*, 1101.

(25) (a) Bedel, S.; Ulrich, G.; Picard, C.; Tisnès, P. *Synthesis* **2002**, *11*, 1564. (b) Ulrich, G.; Bedel, S.; Picard, C.; Tisnès, P. *Tetrahedron Lett.* **2001**, *42*, 6113.

Chart 1

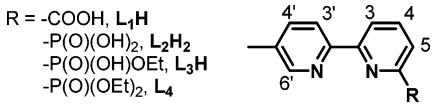

simple synthetic means, allowing further functionalization that would permit several of these tridentate ligands to be conjugated to a preorganized platform.[13a,26] Complexation of lanthanide cations such as europium and terbium gave very stable, water-soluble, and luminescent complexes that can be used as probes for luminescence labeling and time-resolved applications.[27]

This work aims at understanding the varying parameters governing the association of the lanthanide cations with different tridentate ligands based on bipy frameworks and describes the complexation with ligands $\mathbf{L_1}-\mathbf{L_4}$ (Chart 1), based on 2,2′-bipyridines substituted in the 6 position by a carboxylic acid ($\mathbf{L_1}$H), a phosphonic acid ($\mathbf{L_2}H_2$), and monoethyl- ($\mathbf{L_3}$H) or diethyl- ($\mathbf{L_4}$) phosphonic esters. The synthesis and full characterization of the new ligands $\mathbf{L_2}-\mathbf{L_4}$ is described, together with a detailed examination of their acid−base behaviors, their complexation ability toward lanthanide cations in aqueous solutions, and the photophysical properties of the ligands and their complexes.

Experimental Section

Synthesis of the Ligands. Starting Materials and General Procedures. Solvents and reagents were of analytical grade and were used as received. Toluene and $(^i\mathrm{Pr})_2$EtN were distilled from Na and KOH, respectively, under an argon atmosphere immediately prior to use.[28] ^{1}H NMR (200 and 400 MHz), ^{31}P NMR (161.9 MHz), and ^{13}C NMR (50 or 100 MHz) spectra were recorded on Bruker AC200 and AMX400 spectrometers, using perdeuterated solvents as internal standards. FT-IR spectra were obtained from KBr pellets on a Nicolet 210 spectrometer. Fast-atom bombardment (FAB, positive mode) mass spectra were recorded using *m*-nitrobenzyl alcohol as a matrix. 6-Bromo-5′-methyl-2,2′-bipyridine and ligand $\mathbf{L_1}$ were synthesized according to literature procedure.[24c]

Preparation of Ligand $\mathbf{L_4}$. A Schlenk round-bottom flask was charged with 6-bromo-5′-methyl-2,2′-bipyridine (1.00 g, 4 mmol), anhydrous toluene (50 mL), triphenylphosphine (1.00 g, 3.8 mmol), and anhydrous $(^i\mathrm{Pr})_2$EtN (3 mL). After degassing of this solution with argon (30 min), $[Pd(PPh_3)_4]$ (0.46 g, 0.4 mmol) was added as a solid. Then $HP(O)(OEt)_2$ (0.7 mL, 5.07 mmol) was added through a septum and the yellowish solution was heated at 100 °C overnight without any noticeable color change. The solution was allowed to cool to room temperature, and water (50 mL) was added. The solution was then evaporated to dryness. The crude precipitate was extracted three times with dichloromethane, the organic extracts were combined, treated with water (3 × 100 mL), dried over $MgSO_4$, filtered, and evaporated to dryness, and the residue was purified by flash chromatography on silica gel using CH_2Cl_2 with a gradient of methanol (1 to 2%) as the mobile phase. The desired ligand $\mathbf{L_4}$ was recovered as a colorless powder after trituration in hexane, affording 1.00 g (81% yield). ^{1}H NMR ($CDCl_3$, 200 MHz): $\delta = 8.47$ (10 lines multiplet, 2H), 8.36 (d, 1H, $^3J = 8.4$ Hz), 7.23 (9 lines multiplet, 2H), 7.60 (dd, 1H, $^3J = 8.4$ Hz, $^4J = 2.0$ Hz), 4.26 (22 lines multiplets, 4H), 2.38 (s, 3H), 1.36 (t, 6H, $^3J = 7.1$ Hz). ^{13}C{^{1}H} NMR ($CDCl_3$, 100.6 MHz): $\delta = 157.2$ (d, $^2J_{PC} = 22.6$ Hz), 153.0 (d, $J_{PC} = 31.5$ Hz), 150.5, 150.0, 137.9, 137.3 (d, $^3J_{PC} = 12.4$ Hz), 134.4, 127.9 (d, $^2J_{PC} = 25.4$ Hz), 123.3, 121.4, 63.5 (d, $^2J_{PC} = 5.8$ Hz), 18.8, 16.8 (d, $^3J_{PC} = 6.0$ Hz). ^{31}P-{^{1}H} NMR ($CDCl_3$, 161.9 MHz): $\delta = 11.82$ ppm. FT-IR (KBr, cm^{-1}): $\tilde{\nu} = 2975$ (m), 2932 (m), 1639 (m), 1439 (m), 1398 (m), 1384 (m), 1234 (m), 1162 (m), 1089 (m), 1049 (s), 973 (m), 566 (m), 543 (m). FAB$^+$ (*m*-NBA): *m*/*e* 307.2 ([M + H]$^+$, 100%). Anal. Calcd for $C_{15}H_{19}N_2O_3P$ ($M_r = 306.297$): C, 58.82; H, 6.25; N, 9.15. Found: C, 58.62; H, 5.99; N, 9.02.

Preparation of Ligand $\mathbf{L_3}$Na. In a round-bottom flask equipped with an open air condenser, the diester $\mathbf{L_4}$ (0.300 g, 0.98 mmol) was suspended in aqueous NaOH (20 mL, 0.05 N) and heated 1 night at 100 °C. After heating of the sample at reflux, the pH of the remaining clear solution was ca. 7. The solution was evaporated to dryness using a rotavapor and dried under high vacuum for 2 h. The resulting residue was extracted with three portions of dichloromethane, filtered over Celite, and dried over $MgSO_4$ and filtered, and the target ligand was precipitated by slow addition of hexane, affording 0.243 g of the sodium salt (83%) as a white powder. ^{1}H NMR ($CDCl_3$, 200 MHz): $\delta = 7.77$ (broad singlet, 1H), 7.74 (5 lines multiplet, 3H), 7.49 (6 lines multiplet, 1H), 7.30 (5 lines multiplet, 1H), 3.68 (5 lines multiplets, 2H), 2.14 (s, 3H), 0.78 (t, 3H, $^3J = 7.1$ Hz). ^{13}C{^{1}H} NMR (CD_3OD, 100.6 MHz): $\delta = 158.8$ (d, $J_{PC} = 209.9$ Hz), 155.5 (d, $^2J_{PC} = 20.1$ Hz), 153.6, 149.6, 138.2, 136.9 (d, $^3J_{PC} = 10.6$ Hz), 134.5, 126.4 (d, $^2J_{PC} = 22.1$ Hz), 121.7, 121.2, 61.2 (d, $^2J_{PC} = 5.5$ Hz), 17.2, 16.5 (d, $^3J_{PC} = 6.8$ Hz). ^{31}P-{^{1}H} NMR ($CDCl_3$, 161.9 MHz): $\delta = 8.81$ ppm. FT-IR (KBr, cm^{-1}): $\nu = 2976$ (m), 2927 (m), 2889 (m), 1654 (m), 1637 (m), 1560 (s), 1445 (m), 1213 (m), 1090 (s), 1049 (s), 940 (m), 563 (m). ES-MS$^+$ (methanol 120 eV): *m*/*e* 301.1 ([$\mathbf{L_3}$Na + H]$^+$, 100%), 279.1 ([$\mathbf{L_3}$H + H]$^+$, 50%). Anal. Calcd for $C_{13}H_{14}N_2O_3PNa$ ($M_r = 300.225$): C, 52.01; H, 4.70; N, 9.33. Found: C, 51.87; H, 4.51; N, 8.99.

Preparation of Ligand $\mathbf{L_2}H_2$. A Schlenk round-bottom flask was charged with ligand $\mathbf{L_4}$ (0.295 g, 0.98 mmol), anhydrous dichloromethane (10 mL), and trimethylsilyl bromide (1.29 mL, 9.82 mmol) under a continuous flow of argon. This solution was stirred at room temperature for 2 days. During this period a white precipitate appeared. The solid was recovered by filtration through a glass frit and washed with large amounts of anhydrous dichloromethane, yielding 0.210 g of the desired derivative (80% yield). ^{1}H NMR (DMSO-d_6, 300.13 MHz): $\delta = 8.59$ (s, 1H), 8.44 (d, 1H, $^3J = 8.1$ Hz), 8.35 (dd, 1H, $^3J = 7.5$ Hz, $^4J = 1.0$ Hz), 8.02 (10 lines multiplets, 2H), 7.79 (td, 1H, $^3J = 6.0$ Hz, $^4J = 1.0$ Hz), 2.48 (s overlapping with the solvent, 3H). ^{13}C{^{1}H} NMR (DMSO-d_6, 75.5 MHz): $\delta = 158.2$, 155.3, 149.9, 147.1, 142.2, 138.3 (d, $^3J_{PC} = 11.1$ Hz), 136.4, 127.3 (d, $^2J_{PC} = 24.0$ Hz), 122.7 (d, $^2J_{PC} = 20.5$ Hz), 121.4, 18.3. ^{31}P{^{1}H} NMR (DMSO-d_6, 161.9 MHz): $\delta = 7.16$ ppm. FT-IR (KBr, cm^{-1}): $\tilde{\nu} = 2976$ (m), 2897 (w), 1631 (m), 1549 (s), 1447 (m), 1221 (m), 1087 (s), 1049 (s), 1014 (m), 934 (m), 543 (m). FAB$^+$ (*m*-NBA): *m*/*e* 251.2 ([M + H]$^+$, 100%), 234.2 ([M − O], 50%). Anal. Calcd for $C_{11}H_{11}N_2O_3P\cdot H_2O$ ($M_r = 250.051 + 18.015$): C, 49.26; H, 4.89; N, 10.44. Found: C, 49.17; H, 4.80; N, 10.32.

Spectrophotometric Measurements. Analytical grade solvents and chemicals (Fluka AG) were used without further purification. The Tris-HCl buffer solutions 0.1 M in doubly distilled water were obtained by dilution of a 1 M Sigma T 2663 solution. Stock

(26) Ziessel, R. F.; Charbonnière, L. J.; Cesario, M.; Prangé, T.; Guardigli, M.; Roda, A.; van Dorsselaer, A.; Nierengarten, H. *J. Supramol. Chem.* **2003**, *15*, 277.
(27) Weibel, N.; Charbonnière, L. J.; Guardigli, M.; Roda, A.; Ziessel, R. *J. Am. Chem. Soc.* **2004**, *126*, 4888.
(28) Perrin, D. D.; Armarego, W. L. F. In *Purification of Laboratory Chemicals*, 3rd ed.; Pergamon Press: New York, 1988.

solutions of lanthanides were prepared just before use in freshly boiled, doubly distilled water from the corresponding perchlorate salts $Ln(ClO_4)_3 \cdot nH_2O$ (Ln = La, Nd, Eu, Gd, Tb, and Lu; n = 4−6). *Caution! Perchlorate salts combined with organic ligands are potentially explosive and should be handled in small quantities and with adequate precautions.*[29] These salts were prepared from their oxides (Rhône-Poulenc, 99.99%) in the usual way.[30] The concentrations of the solutions were determined by complexometric titrations using a standardized Na_2H_2EDTA solution in urotropine-buffered medium and with xylenol orange as indicator.[31] UV−vis absorption spectra were measured on a Perkin-Elmer Lambda 900 spectrometer using quartz Suprasil cells of 0.2- and 1-cm path length. Spectrophotometric titrations were performed with a J&M diode-array spectrometer (Tidas series) connected to an external computer. All titrations were performed in a thermostated (25.0 ± 0.1 °C) glass-jacketed vessel at μ = 0.1 M (KCl). In a typical experiment for ligands titrations as a function of pH, 50 mL of a 3×10^{-5} M ligand solution was titrated with freshly prepared sodium hydroxide solutions at different concentrations (4, 1, 0.1, and 0.01 M). After each addition of base, the pH of the solution was measured by a KCl-saturated electrode and UV−vis absorption spectra were recorded using a Hellma optrode (optical path length 1 cm) immersed in the thermostated titration vessel and connected to the Tidas spectrometer. The same conditions were used for the titration as a function of pH of stoichiometric 1:1 and 1:3 quantities of $Eu(ClO_4)_3 \cdot nH_2O$ and ligands $\mathbf{L_1}$ and $\mathbf{L_2}$, respectively (see Supporting Information). Solutions were systematically acidified with HCl before metal addition to avoid hydroxide precipitation. Conditional stability constants were determined by titration of the ligands by Ln(III) at fixed pH (0.1 M Tris-HCl buffer, pH 7.45) using the same equipment. In this case, Ln(III) solutions with relative high concentrations were used (5×10^{-3} M as compared to 3×10^{-5} M for ligand solutions) to minimize dilution effects. Factor analysis[32] and mathematical treatment of the spectrophotometric data were performed with the SPECFIT program.[33]

NMR Measurements. 1D ^{1}H and ^{31}P NMR spectroscopy as well as 2D COSY experiments were performed on a Bruker Avance DRX 400 spectrometer at 25 °C. Chemical shifts are given in ppm relative to TMS. All the spectra were recorded in deuterated water (D_2O, 99.9%, Aldrich). Typically, NMR titrations of the ligands as a function of pD were performed using 5 mL of ligand solutions 10^{-2} or 5×10^{-3} M. Variations of the pD were achieved by addition of small volumes of D_2SO_4 (Fluka, puriss) and NaOD (Merck) solutions at different concentrations. The pH values of the solutions were determined with a Metrohm pH-meter (744) equipped with a glass electrode (1 M KCl, 3.8 mm diameter, 150 mm height; Willi Möller AG). The ionic strength was not adjusted. The pD values were calculated as $pD = pH_{meas} + 0.4$.[34] The same method was used for titrating the ligand by Ln(III) ions in a pD range (7.5 ± 0.1) kept constant by additions of small volumes of NaOD or D_2SO_4. Spectra were recorded after pD equilibration. A 1 mL volume of 5×10^{-3} M ligand solutions was typically titrated with 5×10^{-2} M $Ln(ClO_4)_3 \cdot nH_2O$ (Ln = Nd, Lu) solutions in D_2O.

Luminescence Measurements. Low-resolution luminescence measurements (spectra and lifetimes) were recorded on a Fluorolog 3-22 spectrometer from Jobin-Yvon. Emission and excitation spectra were measured in 1-cm path length quartz Suprasil cell at room temperature (25 °C) and corrected for the instrumental function. The temperature was kept constant by using a FL-1027 thermostated cell holder connected to a water bath. Phosphorescence lifetimes (τ) were measured in frozen glycerol/water solutions (10/90%) put into quartz capillaries. They are averages of at least three independent measurements which were made by monitoring the decay at the maxima of the emission spectra, enforcing a 0.05 ms delay. The decays, monoexponential or biexponential, were analyzed with Origin 7.0. Solutions of ligands and of their 1:3 complexes (Ln/L, with Ln = La, Eu, Gd, Tb, and Lu) were prepared in 0.1 M Tris-HCl buffer (pH 7.4). All the measurements were performed on 2×10^{-5} M samples, prepared from stock solutions of ligands $\mathbf{L_1}$-$\mathbf{L_4}$ (10^{-3}−10^{-4} M) and $Ln(ClO_4)_3 \cdot nH_2O$ (~5×10^{-3} M). Luminescence titrations of stoichiometric 1:1 and 1:3 quantities of $Eu(ClO_4)_3 \cdot nH_2O$ and ligands $\mathbf{L_1}$ and $\mathbf{L_2}$, respectively, as a function of pH, were performed simultaneously with the spectrophotometric measurements by transferring 3 mL of the investigated solution into a 1 cm quartz cell (see Supporting Information). Quantum yields (Φ) of europium and terbium complexes in 0.1 M Tris-HCl at room temperature were determined relative to those of europium and terbium tris(dipicolinates): $\Phi(Cs_3[Eu(DPA)_3]) = 13.5\%$[35] and $\Phi(Cs_3[Tb(DPA)_3]) = 22.0\%$;[35] estimated error, ±10%. Quartz Suprasil cells with 0.2-cm path length were used for these measurements. The numbers of coordinated water molecules (q) for the Eu and Tb complexes were calculated from the equation $q = A(\tau^{-1}_{H_2O} - \tau^{-1}_{D_2O} - k_{corr})$, where τ_{H_2O} and τ_{D_2O} are the lifetimes in H_2O and D_2O, respectively; for europium, $A = 1.11$ and $k_{corr} = 0.31$ ms^{-1} [7c] or $A = 1.2$ and $k_{corr} = 0.25$ ms^{-1},[7e] and for terbium, $A = 5.0$ and $k_{corr} = 0.06$ ms^{-1}.[7e]

Results and Discussion

Synthesis and Characterization of the Ligands. As previously described for the synthesis of $\mathbf{L_1}$,[24c] ligands $\mathbf{L_2}$−$\mathbf{L_4}$ were obtained starting from 6-bromo-5′-methyl-2,2′-bipyridine. The synthesis of the (diethoxyphosphoryl)-bipyridine derivative $\mathbf{L_4}$ was inspired by a synthetic protocol previously reported by Odobel and co-workers.[36] Hünig's base was used to quench the nascent hydrobromic acid, and palladium(0) to promote the cross-coupling reaction with diethyl phosphite.[37] To increase the efficiency of the reaction a large excess of triphenylphosphine was added, as previously reported,[36] and average yields amounting to 80% were obtained. Highly selective hydrolysis of one ethyl ester group of the phosphonate was accomplished in water under reflux with stoichiometric amounts of NaOH. The reaction is easily followed by thin-layer chromatography, and $\mathbf{L_3}$ was isolated in 83% yield. Total cleavage of both ester functions to give $\mathbf{L_2}$ was achieved with trimethylsilyl bromide in dichloromethane as previously reported.[38] In our case this is a convenient protocol because the phosphonic acid precipitates without the need for additional purification. The four ligands

(29) (a) Wolsey, W. C. *J. Chem. Educ.* **1973**, *50*, A335. (b) Raymond, K. N. *Chem. Eng. News* **1983**, *61*, 4.
(30) Desreux, J. F. In *Lanthanide Probes in Life, Chemical and Earth Sciences, Theory and Practice*; Bünzli, J.-C. G., Choppin, G. R.. Eds.; Elsevier Science BV: Amsterdam, 1989; Chapter 2.
(31) Schwarzenbach, G. *Complexometric Titrations*; Chapman & Hall: London, 1957.
(32) Malinowski, E. R.; Howery, D. G. *Factor Analysis in Chemistry*; Wiley: New York, 1980.
(33) (a) Gampp, H.; Maeder, M.; Meyer, C. J.; Zuberbühler, A. D. *Talanta* **1986**, *33*, 943. (b) Gampp, H.; Maeder, M.; Meyer, C. J.; Zuberbühler, A. D. *Talanta* **1985**, *32*, 257.
(34) Mikkelsen, K.; Nielsen, S. O. *J. Phys. Chem.* **1960**, *64*, 632.
(35) Chauvin, A.-S.; Gumy, F.; Imbert, D.; Bünzli, J.-C. G. *Spectrosc. Lett.* **2004**, *37*, in press.
(36) Penicaud, V.; Odobel, F.; Bujoli, B. *Tetrahedron Lett.* **1998**, *39*, 3689.
(37) Hirao, T.; Msunaga, T.; Ohshiro, Y.; Agawa, T. *Synthesis* **1981**, 56.
(38) Montalti, M.; Wadhwa, S.; Kim, W. Y.; Kipp, R. A.; Schmehl, R. H. *Inorg. Chem.* **2000**, *39*, 76.

Table 1. Acidity Constants of Ligands $\mathbf{L_1}$−$\mathbf{L_4}$ as Obtained by UV−Vis Absorption Spectroscopy

	pK_{a_1}	pK_{a_2}	pK_{a_3}	pK_{a_4}
$\mathbf{L_1}$	−0.8/−0.9	2.79(5)	5.18(2)	
$\mathbf{L_2}$	−0.9/−1.0	3.06(5)	5.04(2)	7.11(1)
$\mathbf{L_3}$	−0.9/−1.0	2.98(5)	5.42(1)	
$\mathbf{L_4}$	−0.8/−0.9	4.17(1)		

exhibit well-resolved NMR spectra (^{1}H, ^{13}C, and ^{31}P) and were unambiguously characterized by FT-IR, FAB-MS or ES-MS, and elemental analysis. The fingerprint of the IR spectra is the presence of strong stretching vibration of ν_{P-O} at 1049 cm^{-1} as well as the bending vibration of the δ_{O-P-O} in the 540−566 cm^{-1} range. These assignments are in keeping with previous measurements performed on related derivatives.[37,39]

Determination of pK_a Values of the Ligands. In very acidic medium, bipyridine exists in a diprotonated form[40] and the corresponding dissociation constants are −0.52 and 4.45.[40,41] To establish the first pK_a values for ligands $\mathbf{L_1}$−$\mathbf{L_4}$, UV−vis spectra were measured in solutions prepared from fuming HCl with calculated exact pH values in the range −1.09 to +1.04. At the lowest pH value (−1.09), the absorption spectra of the ligands are dominated by a large band around 300 nm, assigned to the B[42] (or π_1) $\pi \rightarrow \pi^*$ transition. Upon increase of the pH to nearly −0.5, the maximum of this band undergoes a small bathochromic shift to ca. 308 nm and a second absorption band arises at 250 nm, attributed to the A[42] (or π_2[41]) $\pi \rightarrow \pi^*$ transition. These two absorption bands and their energy levels point to the presence of a monoprotonated bipy system in a cis conformation.

From the UV−vis spectra at these low pH values, it was possible to estimate the first pK_a values (the ligands being not totally protonated at pH = −1.09) (see Table 1), which are in reasonable agreement with the one reported for unsubstituted bipy.

In the pH range extending from 1.20 to 10.00, the evolution of the absorption spectra was monitored in water and is represented in Figure 1 for $\mathbf{L_2}$ (see also Figures S1−S3 for $\mathbf{L_1}$, $\mathbf{L_3}$, and $\mathbf{L_4}$, Supporting Information). Fitting the results gives the pK_a values listed in Table 1. The calculated spectra for the different ligands in their varying protonation states are very informative with respect to the assignment of the protonation sites (Figures S4 and S5, Supporting Information). For $\mathbf{L_1}$, $\mathbf{L_3}$, and $\mathbf{L_4}$, the most important variations in the spectra are those related to the highest pK_a values. For pH increases around these pK_a values, the two bands associated with the $\pi \rightarrow \pi^*$ transitions sustain a hypsochromic shift, in line with a second deprotonation of the bipy rings and a concomitant cis−trans isomerization.[40,41] The second pK_a values for ligands $\mathbf{L_1}$ and $\mathbf{L_3}$ can therefore be connected to the deprotonation of the carboxylic acid and

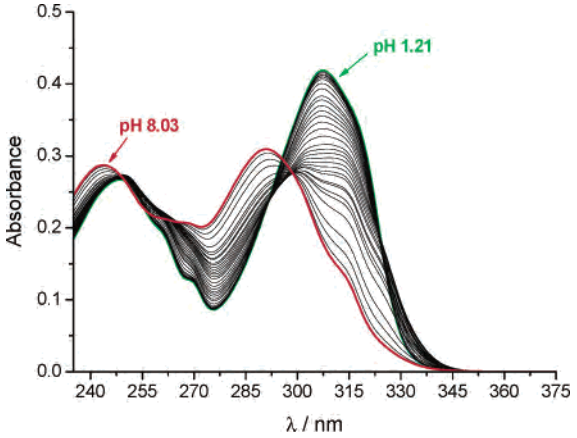

Figure 1. UV−vis absorption spectra of $\mathbf{L_2}$ at pH varying from 1.21 to 8.03.

of the monoethyl phosphonic acid, respectively, as subsequently confirmed by ^{1}H and ^{31}P NMR spectroscopy (vide infra). Comparison of the pK_a values corresponding to the deprotonation of the bipy moieties with the one of bipy (pK_a = 4.45)[41] shows $\mathbf{L_4}$ to be more acidic than the reference compound, as anticipated on the basis of the electron-withdrawing character of the diethyl ester phosphonic acid function. On the other hand, pK_a values for $\mathbf{L_1}$ and $\mathbf{L_3}$ indicate an increased basicity that is related to the electrostatic stabilization due to the neighboring carboxylate and monoethyl phosphonate functions, respectively.

The case of $\mathbf{L_2}$ is somewhat more complicated as the changes observed in the two main absorption bands of the UV−vis absorption spectra occur in the pH range of the last two deprotonation steps (formally: $\mathbf{L_2}H_2 \rightleftarrows \mathbf{L_2}H^- \rightleftarrows \mathbf{L_2}^{2-}$). The calculated spectra of $\mathbf{L_2}H^-$ (Figure S5, Supporting Information) show a large broadening of the low-energy absorption band (band B) but neither net hypsochromic shifts nor those for the A band. It is only when the final deprotonation occurred, leading to $\mathbf{L_2}^{2-}$, that these two bands are shifted to higher energy. On the basis of literature data on phosphonic acids (for example, $C_6H_5PO(OH)_2$, pK_a = 1.68 and 7.02),[43] and in keeping with the attributions made for $\mathbf{L_1}$, $\mathbf{L_3}$, and $\mathbf{L_4}$, one can reasonably assign the second deprotonation step of $\mathbf{L_2}$ (pK_{a2} = 3.06) to the deprotonation of the phosphonic acid, while the third pK_a at 5.04 represents deprotonation of the bipy core and the fourth one (pK_a = 7.11) is correlated to the last deprotonation of the phosphonic acid. It is then surprising to consider that the deprotonation of the bipy core is not accompanied by the classical hypsochromic shift in the UV−vis absorption spectra, which is usually associated with the cis−trans isomerization. It is likely that a tight intramolecular H-bonding between the protonated phosphonic acid and the nitrogen lone pairs of the bipy unit is occurring, as sketched in Scheme 1.

Although the third deprotonation occurs on the bipy unit, the vicinity of the proton of the phosphonic acid also accounts for an intramolecular H-bonding interaction, which

(39) Nakamoto, K. In *Infrared and Raman Spectra of Inorganic and Coordination Compounds*, 4th ed.; Wiley-Interscience: New York, 1986; p 168.
(40) Westheimer, F. H.; Benfey, O. T. *J. Am. Chem. Soc.* **1956**, *78*, 5309.
(41) Nakamoto, K. *J. Phys. Chem.* **1960**, *64*, 1420.
(42) Krumholz, P. *J. Am. Chem. Soc.* **1951**, *73*, 3487.
(43) Wozniak, M.; Nowogrocki, G. *J. Chem. Soc., Dalton Trans.* **1981**, 2423.

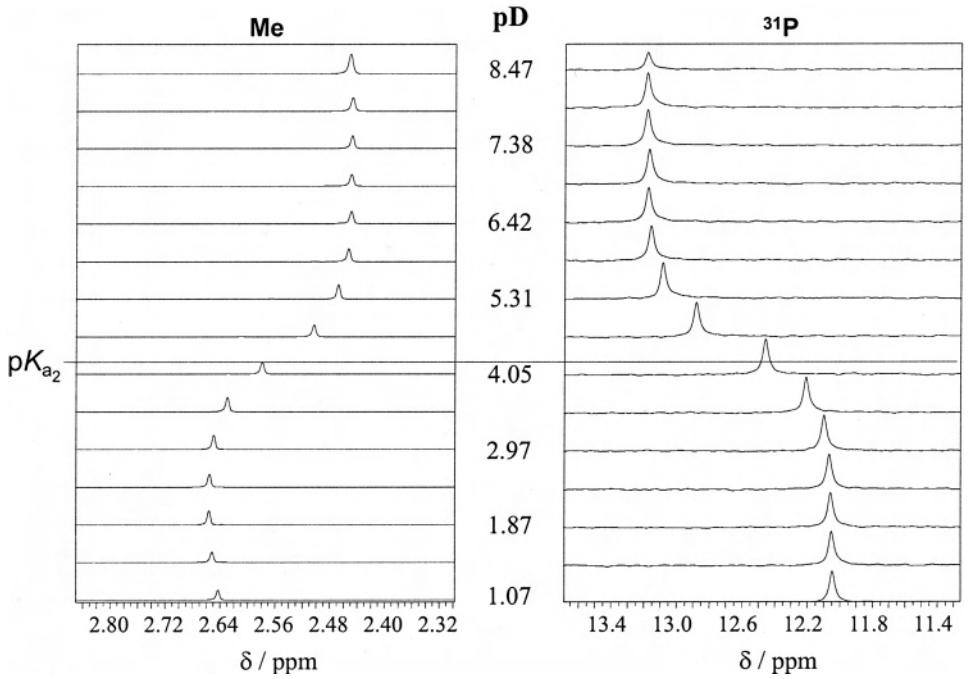

Figure 2. Evolution of the chemical shift of the methyl group (left) and of the phosphorus atom (right) of $\mathbf{L_4}$ as a function of pD in D_2O.

Scheme 1

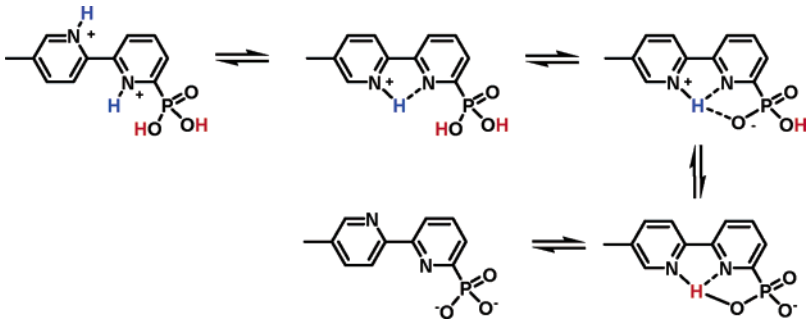

keeps on stabilizing the cis form, thereby maintaining the corresponding $\pi \rightarrow \pi^*$ transitions at low energies. It is only when this proton is removed at higher pH values that the nitrogen lone pair repulsion becomes large enough to induce the hypsochromic shift. A similar behavior is not observed for the other ligands as no H-bonding interaction can stabilize the nonprotonated bipy subunit.

The pK_a assignment was further substantiated by ^{1}H and ^{31}P NMR experiments in D_2O, in which the evolution of the chemical shifts of the proton or phosphorus atoms was monitored as a function of pD (Figures S6−S8, Supporting Information). Interpretation of the results must be handled with care as the evolution of the chemical shifts results from changes in the electronic distribution within the molecule and from environmental factors resulting from potential geometric reorganization. The methyl group in 5′ position of the bipy moiety appears as a very good probe as its position, at the periphery of the molecule and on the C−*C* axis joining the pyridyl rings, makes it relatively insensitive to geometrical changes within the molecule such as cis−trans isomerization.

Figure 2 shows the evolution of the chemical shifts of these protons in $\mathbf{L_4}$ as a function of pD. An upfield shift is clearly observed for pD values in the range of pK_{a2}, showing this signal to be very sensitive to the deprotonation of the bipy. The section of the spectra corresponding to the aromatic protons is also greatly modified in this pD range. A full attribution of the aromatic protons was possible thanks to 2D COSY experiments and is presented in Figure 3.

Increasing pD values leads to a general upfield shift of all aromatic protons (Table 2). This shift is more pronounced for the protons belonging to the methyl-functionalized pyridine ring compared to the second pyridine moiety. Analysis of these shifts for H_4 and $H_{4'}$, both in para positions of the nitrogen atom, indicates that in the protonated form of $\mathbf{L_4}$ the proton is mainly localized on the methylated ring. The increased basicity of the latter is to be related to the presence of an electron-donating methyl group, in opposition to the electron-withdrawing effect of the phosphonic diester function on the other ring. Interestingly, in this same pD range, the chemical shift of the phosphorus atom also changes but to lower field (Figure 2), indicating that even if the phosphonic diester is not directly implied in the protonation mechanism, it suffers large electronic or geometric reorganization upon deprotonation.

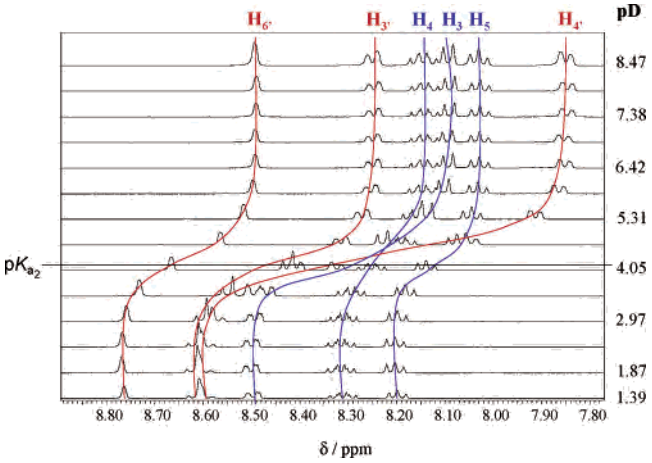

Figure 3. Evolution of the ^{1}H NMR spectra of $\mathbf{L_4}$ in the aromatic range as a function of pD in D_2O.

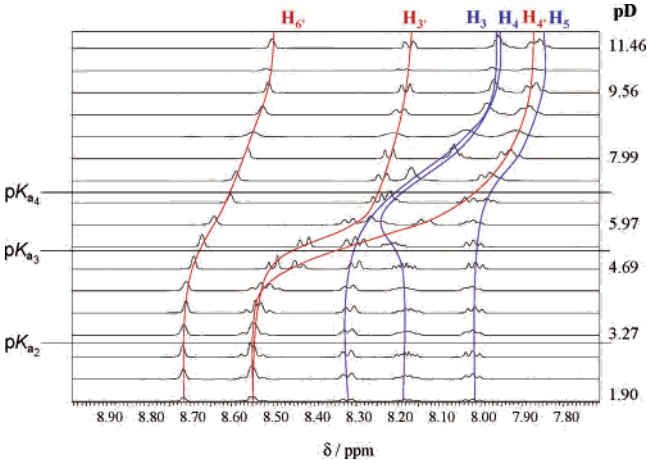

Figure 4. Evolution of the ^{1}H NMR spectra of $\mathbf{L_2}$ in the aromatic range as a function of pD in D_2O.

Table 2. Variations of the Chemical Shifts of the Proton and Phosphorus Atoms of the Ligands between Acidic and Basic Water Solutions

	H_3	H_4	H_5	$H_{3'}$	$H_{4'}$	$H_{6'}$	Me	P
$\mathbf{L_1}$[a]	−0.46	−0.30	−0.31	−0.28	−0.71	−0.28	−0.20	
$\mathbf{L_2}$[b]	−0.37	−0.27	−0.16	−0.37	−0.68	−0.22	−0.14	+0.5[e]
$\mathbf{L_3}$[c]	−0.23	−0.14	−0.14	−0.40	−0.69	−0.22	−0.19	+1.1
$\mathbf{L_4}$[d]	−0.40	−0.16	−0.17	−0.36	−0.73	−0.27	−0.21	+1.1

[a] $\Delta\delta = \delta_{pD=1.26} - \delta_{pD=10.60}$ in ppm. [b] $\Delta\delta = \delta_{pD=1.90} - \delta_{pD=11.46}$ in ppm. [c] $\Delta\delta = \delta_{pD=1.13} - \delta_{pD=9.76}$ in ppm. [d] $\Delta\delta = \delta_{pD=1.87} - \delta_{pD=8.47}$ in ppm. [e] $\Delta\delta_{max} = +2.0$ ppm between pD = 6.60 and pD = 11.46.

For ligands $\mathbf{L_1}$ and $\mathbf{L_3}$, bearing monoionizable functions, the same overall behavior as that of $\mathbf{L_4}$ is observed. Increasing the pD value leads to an upfield shift of all protons, and this shift occurs in the pD range corresponding to pK_{a3}, at which the bipy loses its proton. As for $\mathbf{L_4}$, the main shifts affect the aromatic protons of the methyl functionalized pyridine (see Figures S6−S8, Supporting Information). In the case of $\mathbf{L_3}$, the variations of the ^{31}P chemical shifts is also observed in the pD range corresponding to deprotonation of the bipy around pK_{a3} (Figure S8, Supporting Information). It is surmised that deprotonation of the phosphonic monoester does not have a great influence on the δ value (as observed for the first deprotonation of $\mathbf{L_2}$; vide infra), whereas the cis−trans isomerization accompanying the bipy deprotonation produces a large downfield shift, as observed for $\mathbf{L_4}$.

The situation is far more complicated for $\mathbf{L_2}$ (Figure 4). For pD values ranging from 1.90 to 4.0, corresponding to the pK_{a2} assigned to the first deprotonation of the phosphonic acid, no change occurs in the chemical shifts, neither for proton or for phosphorus. When the pD values reach those around pK_{a3}, assigned to the deprotonation of the bipy unit (Scheme 1), upfield shifts begin to be important for the methyl functionalized pyridyl group and for the phosphorus atom. At this stage, H_4 and H_5 are very little perturbed and H_3 is shifted downfield ($\Delta\delta = +0.06$ ppm). An upfield shift of H_3, H_4, and H_5 requires pD values close to pK_{a4}. The chemical shifts of the other protons keep on shifting upfield, whereas $\delta(^{31}P)$ reverses its trend and moves downfield to ca. +6.7 ppm (Figure S7, Supporting Information). This behavior can be reasonably well explained on the basis of the structures presented in Scheme 1.

For all the studied ligands, the main changes evidenced around pH values close to pK_{a3} arise for the methyl-functionalized pyridine ring. However, deprotonation of the bipyridine in $\mathbf{L_2}$ is not accompanied by cis−trans isomerization (see UV−vis titration data). The protons of the phosphorylated ring (H_3−H_5) are then little affected, except for a downfield shift of H_3 resulting from a modification of the interannular dihedral angle and from the electronic effect of the phosphonic acid in the *para* position. Finally, the second deprotonation of the phosphonic acid breaks the H-bonding pattern, resulting in cis−trans isomerization of the bipy framework, leading in an upfield shift for all protons and to a sizable downfield shift for the phosphorus atom ($\Delta\delta = 2.0$ ppm), as previously observed for the other ligands.

Stoichiometry and Stability of the Ln Complexes with Ligands $\mathbf{L_1}$−$\mathbf{L_4}$. We have turned to UV−vis spectrophotometric titrations to get insight into the interaction between the lanthanide ions and the investigated ligands. Increasing amounts of lanthanide perchlorates (Ln = La, Nd, Eu, Lu) were added to aqueous 3×10^{-5} M solutions of the ligands, buffered at pH = 7.4 with Tris-HCl, up-to-a ratio Ln/L equal to 2:1. At this pH, all the ligands are in their fully deprotonated form, thereby simplifying the fitting procedure performed with a nonlinear least-squares algorithm implemented in the Specfit software.[33]

In the case of $\mathbf{L_4}$, additions of up to 4 equiv of europium did not result in any significant changes in the absorption spectra, indicative of a very weak interaction. For ligand $\mathbf{L_3}$, the addition of aliquots of europium perchlorate resulted in the stepwise displacement of the absorption maximum from 287 nm for the free ligand up to 304 nm in the presence of 4 equiv of europium. This bathochromic shift is in line with the cis−trans isomerization occurring upon complexation. Surprisingly however, the spectra keep on evolving after addition of 1 equiv of metal, and they cannot be satisfactorily fitted with simple models including $Eu_X(\mathbf{L_3})_Y$ species, X and Y being integers. We anticipate that this behavior is indicative of the formation of polymetallic species, as was evidenced by the FAB-MS spectrum of the solid isolated from a two

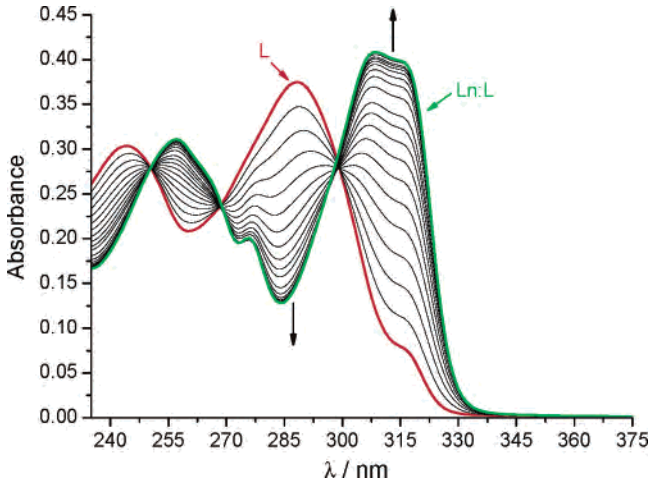

Figure 5. UV−vis absorption spectra of a solution of $\mathbf{L_1}$ in water (pH = 7.4, Tris-HCl) upon addition of increasing amounts of europium, from 0 to 4 equiv.

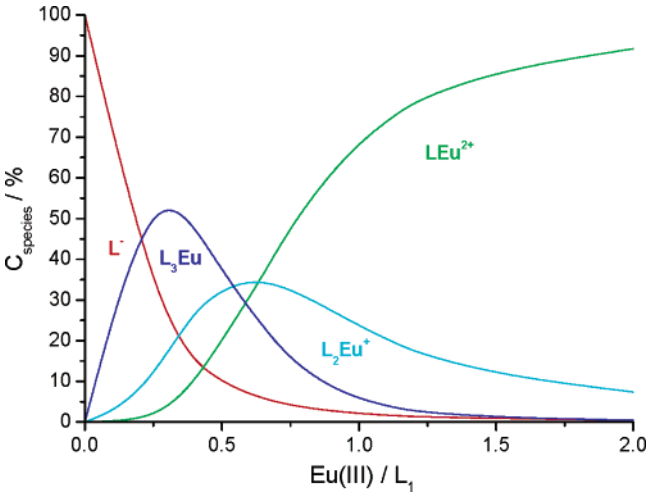

Figure 6. Relative concentrations of the species formed during the titration of $\mathbf{L_1}$ by europium in water (pH = 7.4, Tris-HCl).

Table 3. log β_n Values for Titration of Ligands $\mathbf{L_1}$ and $\mathbf{L_2}$ with Lanthanide Cations in Water (pH = 7.4, Tris-HCl)

ligand	log β_i	La	Nd	Eu	Lu
$\mathbf{L_1}$	log β_1	5.8(1)	6.2(2)	6.8(2)	6.3(1)
	log β_2	10.6(1)	11.4(2)	12.2(2)	11.3(1)
	log β_3	14.6(−)[a]	16.0(2)	17.6(2)	15.8(1)
$\mathbf{L_2}$	log β_1	7.3(2)	8.4(5)	8.5(4)	7.4(2)
	log β_2	12.7(2)	14.7(1)	14.1(4)	12.6(2)
	log β_3	17.7(2)	20.3(5)	19.4(4)	18.0(2)

[a] Constrained value.

to one mixture of $\mathbf{L_3}$ and $Eu(NO_3)_3$ (Figure S9, Supporting Information).

In the case of ligands $\mathbf{L_1}$ and $\mathbf{L_2}$, addition of lanthanide perchlorate also resulted in a bathochromic shift of the absorption maxima from 244 and 288 nm for the free ligands to 257 and 308 nm, respectively, upon addition of 1 equiv of metal (Ln = Eu, L = $\mathbf{L_1}$; Figure 5). An evolving factor analysis indicated the presence of three new absorbing species during the titration and the data could be satisfyingly fitted to the following model (i = 1, 2; charges are omitted for the sake of simplicity):

$$\mathrm{Ln} + \mathbf{L}_i \leftrightarrows [\mathrm{Ln}\mathbf{L}_i] \qquad \log \beta_1 = \frac{[\mathrm{Ln}\mathbf{L}_i]}{[\mathrm{Ln}][\mathbf{L}_i]} \qquad (1)$$

$$\mathrm{Ln} + 2\mathbf{L}_i \leftrightarrows [\mathrm{Ln}(\mathbf{L}_i)_2] \qquad \log \beta_2 = \frac{[\mathrm{Ln}(\mathbf{L}_i)_2]}{[\mathrm{Ln}][\mathbf{L}_i]^2} \qquad (2)$$

$$\mathrm{Ln} + 3\mathbf{L}_i \leftrightarrows [\mathrm{Ln}(\mathbf{L}_i)_3] \qquad \log \beta_3 = \frac{[\mathrm{Ln}(\mathbf{L}_i)_3]}{[\mathrm{Ln}][\mathbf{L}_i]^3} \qquad (3)$$

Values of log β_n (n = 1−3) are gathered in Table 3 while Figure 6 represents the evolution of the relative concentrations of the species formed during the titration.

A small discrimination effect along the lanthanide series is observed for both $\mathbf{L_1}$ and $\mathbf{L_2}$, with the highest stability for europium, around the middle of the series. Comparing the complexation ability of $\mathbf{L_2}$ relative to $\mathbf{L_1}$, we find $\Delta\log \beta_3 = \log \beta_{3(\mathbf{L_2})} - \log \beta_{3(\mathbf{L_1})}$ equal to 3.1, 4.3, 1.8, and 2.2 for La, Nd, Eu, and Lu, respectively. The stronger Ln−$\mathbf{L}_i$ interaction observed with the phosphonate function is principally, but not only, due to its dianionic nature at pH = 7.4. It mainly arises from the first complexation step, with $\Delta\log \beta_1 = \log \beta_{1(\mathbf{L_2})} - \log \beta_{1(\mathbf{L_1})}$ equal to 1.5, 2.2, 1.7, and 1.1 for La, Nd, Eu, and Lu, respectively. Comparison of the stepwise association constants ($K_2 = \beta_2/\beta_1$ and $K_3 = \beta_3/\beta_2$) indicates that the driving forces for the complexation of the second ligand are still mostly in favor of $\mathbf{L_2}$ but to a much lesser extent, with the exception of Lu; this is no more the case for the binding of the third ligand. It is surmised that this reduced attractiveness of $\mathbf{L_2}$ over $\mathbf{L_1}$ is due to a decrease in electrostatic interactions.

To confirm the spectrophotometric data, complexation of $\mathbf{L_1}$ and $\mathbf{L_2}$ with Lu and Nd was also followed by ^{1}H NMR experiments in which the spectra of 5×10^{-3} M solutions of the ligands in D_2O were monitored as a function of added aliquots of cations, the pD being maintained at 7.5 with NaOD or D_2SO_4 (see Figure 7 for the titration of $\mathbf{L_1}$ with Lu). Substantial broadening of the ligand spectrum is observed upon addition of the metal ion, up to a Ln/L ratio of 1:3. At this stage, and for all titrations performed, a precipitate formed, preventing any quantitative treatment, which disappeared after addition of further quantities of cation. Despite the probable presence of facial and meridional isomers for the $[Lu(\mathbf{L_1})_3]$ complex, the spectra only display 6 signals in the aromatic range, indicating that either a single isomer is present or that the exchange between the two isomers is rapid on the NMR time scale. When the Ln/L ratio reaches 2:1, a new, possibly polymetallic, species forms that was not observed during the UV−vis titration performed at lower concentrations.

Since high thermodynamic stability is a stringent requirement for the use of luminescent probes in biomedical analyses, we have compared the stability of the complexes with $\mathbf{L_1}$ and $\mathbf{L_2}$ to those with other ligands, using their pM values, defined as pM = −log [Ln_{free}] for a total concentration of 10^{-6} M in metal ion and 10^{-5} M in ligand at pH = 7.4.[44] Taking into account the speciation of the complexes (Figures S10 and S11, Supporting Information) and the pK_a values of the ligands, pEu values of 12.0 and 12.3 were

Table 4. Energies of the Singlet and Triplet States of the Ligands in the Ln($\mathbf{L}_i$)$_3$ Complexes 2×10^{-5} M in 0.1 M Tris-HCl

Ln	L	$E(^1\pi\pi^*)/cm^{-1}$ [a]	$E(^3\pi\pi^*)/cm^{-1}$ [b]	$\Delta E/cm^{-1}$ [c]	τ/ms[d]
La	$\mathbf{L_1}$	*29 050*	*21 600*, 22 950		51(2), 272(25)
	$\mathbf{L_2}$	*29 500*	*21 750*, 25 150		73(2), 395(25)
Lu	$\mathbf{L_1}$	*28 800*	*21 350*, 22 600		74(2), 380(38)
	$\mathbf{L_2}$	*29 500*	*25 200*		65(3), 340(44)
Gd	$\mathbf{L_1}$	*28 800*	*21 350*, 22 800		6.53(5)
	$\mathbf{L_2}$	*29 700*	*21 250*, 25 400		
Eu	$\mathbf{L_1}$[e]	*28 400*	*21 700*, 22 950	5650	0.89(1)
	$\mathbf{L_2}$[e]	*29 850*	*22 900*, 25 300	8000	0.59(1)
	$\mathbf{L_3}$	*29 750*	*22 100*, 25 650	8350	130(5), 682(62)
	$\mathbf{L_4}$	*29 750*	*22 200*, 25 400	8100	112(3), 660(37)
Tb	$\mathbf{L_1}$[e]	*28 550*	*21 550*, 22 950	2500	2.22(2)
	$\mathbf{L_2}$[e]	*29 850*	*23 150*, 25 150	4700	1.82(2)

[a] From fluorescence spectra at 295 K, maximum of the band envelope. [b] From phosphorescence spectra at 77 K. Maxima of the band envelopes are italicized; the other figure correspond to the energy of the 0-phonon transition. [c] Energy difference between the 0-phonon $^3\pi\pi^*$ ligand level and the Ln(^5D_J) level, with $E(^5D_0) = 17\ 300\ cm^{-1}$ and $E(^5D_4) = 20\ 450\ cm^{-1}$. [d] Lifetimes at 77 K of the ligand $^3\pi\pi^*$ states and, for the Eu and Tb complexes with $\mathbf{L_1}$ and $\mathbf{L_2}$, of the ^5D_J excited levels (analysis on the $^5D_0 \rightarrow {}^7F_2$ and $^5D_4 \rightarrow {}^7F_5$ transitions). [e] Faint emission from the ligand $^1\pi\pi^*$ and $^3\pi\pi^*$ states.

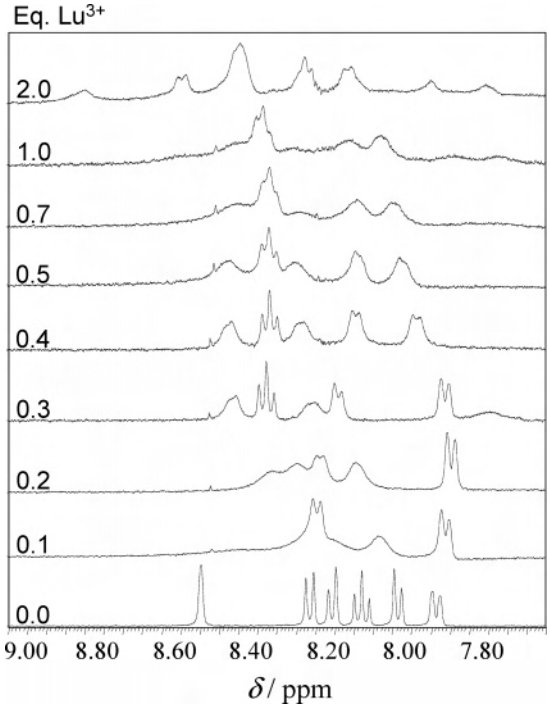

Figure 7. Evolution of the ^{1}H NMR spectra of $\mathbf{L_1}$ in D_2O as a function of added Lu (pD = 7.5).

obtained for $\mathbf{L_1}$ and $\mathbf{L_2}$, respectively. They compare relatively favorably with values found for similar tridentate ligand, such as dpa (dipicolinic acid, pEu = 12.2) but not with those of ligands with higher denticity such as edta (ethylenediaminetetraacetic acid, pEu = 15.6), dtpa (diethylenetriaminepentaacetic acid, pEu = 19.6), or dota (1,4,7,10-tetraazacyclododecanetetraacetic, pEu = 21.2), for which the entropic effect of the functionalized arms induces a stronger complexation effect. This is encouraging, given the simplicity of the ligand design and, moreover, its ability to be easily grafted on more elaborate architectures.[13a,24−27]

Photophysical Properties. Ligand-Centered Luminescence. The absorption spectra of the ligands feature two main bands (with additional shoulders) located around 40 000 and 33 000 cm^{-1} and assigned to $\pi \rightarrow \pi^*$ transitions mainly located on the pyridine units for the latter while the former contains substantial contributions from the carboxylic ($\mathbf{L_1}$) or phosphoryl groups ($\mathbf{L_2}-\mathbf{L_4}$), according to calculations performed with the CAChe Pro 6.0 program package for Windows (Fujitsu Ltd., 2000−2002). The high-energy band is somewhat blue shifted (160−820 cm^{-1}) in going from the acidic to the basic forms of the ligands, except for $\mathbf{L_1}$, for which it is red shifted (480 cm^{-1}). The low-energy absorption is more sensitive to the acid/base change, undergoing an hypsochromic shift of about 900 cm^{-1} for $\mathbf{L_1}$ and around 1800−2150 cm^{-1} for $\mathbf{L_2}-\mathbf{L_4}$ (Table S1, Supporting Information). Under excitation at 37 880 cm^{-1}, an emission band appears, centered at 29 000−30 000 cm^{-1}, which disappears upon enforcement of a time delay and consequently assigned as arising from a $^1\pi\pi^*$ state. At low temperature (77 K, in solutions containing 10% glycerol), a second emission band appears in the range 22 000−23 000 cm^{-1}, displaying a biexponential decay in the 60−140 and 330−740 ms ranges, respectively, and corresponding to phosphorescence from triplet states. It is noteworthy that the band is structured and extends down to about 16 000 cm^{-1}. The yield for the intersystem crossing has been estimated from the relative band area of the $^1\pi\pi^*$ and $^3\pi\pi^*$ emission at 77 K to be roughly 50, 60, 75, and 85% for $\mathbf{L_1}-\mathbf{L_4}$, respectively.

The ligand-centered luminescence of the Ln($\mathbf{L}_i$)$_3$ complexes (Ln = La, Eu, Gd, Tb, Lu) displays essentially the same features as the free ligand luminescence (Table 4). In the case of $\mathbf{L_1}$, the energies of both the singlet and triplet states are slightly red shifted (250−650 cm^{-1}). The vibrational progression on the emission band of the triplet state is better resolved and amounts to 1360 ± 50 cm^{-1} for Gd, corresponding to a ring breathing mode. The $^1\pi\pi^*$ and $^3\pi\pi^*$ emission of the Eu^{III} and Tb^{III} complexes are extremely faint, and the characteristic narrow emission lines of the metal ions are observed, reflecting an efficient ligand-to-metal energy transfer (Figure S12, Supporting Information). The situation is similar for the complexes with $\mathbf{L_2}$ (Figure 8), but the energy shift of the ligand excited levels is smaller than with $\mathbf{L_1}$ (0−300 cm^{-1}). On the other hand, the solutions containing a 1:3 Eu/L molar ratio with L = $\mathbf{L_3}$ and $\mathbf{L_4}$ only display faint metal-centered luminescence (Figure S13, Supporting

(44) Raymond, K. N.; Müller, G.; Matzanke, F. *Top. Curr. Chem.* **1984**, *123*, 49.

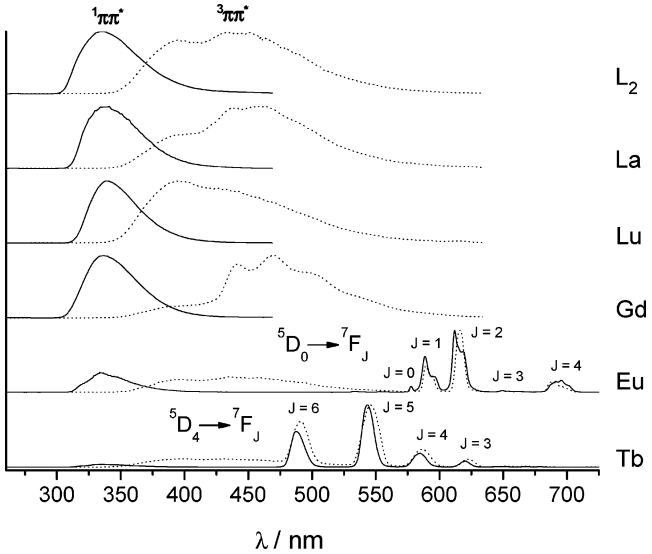

Figure 8. Luminescence spectra of $\mathbf{L_2}$ and its 1:3 complexes at room temperature (solid line, $[\mathbf{L_2}] = 6 \times 10^{-5}$ M in 0.1 M Tris-HCl, pH = 7.4, without time delay) and 77 K (dotted line, in H_2O containing 10% glycerol, with a 0.05 ms time delay).

Table 5. Number of Water Molecules Bound in the Inner Coordination Sphere of the Eu^{III} and Tb^{III} Ions in Solutions at pH = 7.4 and Containing a Ln/L Ratio Equal to 1:3

Ln	L	$k_{obs}(H_2O)/ms^{-1}$	$k_{obs}(D_2O)/ms^{-1}$	$q \pm 0.3^a$	$q' \pm 0.3^b$
Eu	$\mathbf{L_1}$	2.080	0.352	1.6	1.8
	$\mathbf{L_2}$	1.820	0.448	1.2	1.4
	$\mathbf{L_3}$	2.780	0.336	2.4	2.6
	$\mathbf{L_4}$	5.880	0.344	5.9	6.4
Tb	$\mathbf{L_1}$	0.909	0.543		1.5
	$\mathbf{L_2}$	0.926	0.571		1.5

[a] From Horrocks' equation;[7c] $q(Eu) = 1.11(\Delta k - 0.31)$. [b] From Parker's equations:[7e] $q'(Eu) = 1.2(\Delta k - 0.25)$ and $q'(Tb) = 5.0(\Delta k - 0.06)$.

Information), in line with the weak metal−ligand interaction evidenced by the spectrophotometric and NMR titrations.

Metal-Centered Luminescence. The metal-centered luminescence spectra reflect low-symmetry species. The relevant data have essentially been used to determine the number of bound water molecules in the inner coordination sphere, as well as the quantum yield of this luminescence upon ligand excitation.

The number q of bound water molecules in the inner coordination sphere of Eu^{III} and Tb^{III} has been determined by the methods of Horrocks[7c] and Parker and co-workers[7e] by measuring the Eu($^5D_0$) and Tb($^5D_4$) lifetimes of solutions containing $[Ln]_t = 2 \times 10^{-5}$ M and $[L]_t = 6 \times 10^{-5}$ M (pH = 7.4, Tris/HCl buffer). Data are reported in Table 5.

For Eu^{III} both sets of q values are in good agreement. One notes that the luminescence decays are single exponential and that fractional values tend to be obtained, which could be explained by the presence of equilibria between different species. Indeed, under the experimental conditions used, with $[Eu]_t = 2 \times 10^{-5}$ M, at physiological pH, the speciation is as follows: 10.8, 26.1, and 63.1% of 1:1, 1:2, and 1:3 species for $\mathbf{L_1}$, while the corresponding data are 8.2, 31.5, and 60.3% for $\mathbf{L_2}$. The large number of water molecules found for the solution with $\mathbf{L_4}$ points again to a weak Ln−L interaction with this ligand.

Table 6. Absolute Quantum Yields (%) and Observed Luminescence of the Eu^{III} and Tb^{III} Ions in Solutions at pH = 7.45 with a Ln/L Ratio Equal to 1:3

				Q_{tot}^{Ln}/%		
Ln	L		τ_{obs}/ms	$[Ln]_t = 2 \times 10^{-5}$ M		$[Ln]_t = 8 \times 10^{-5}$ M
Eu	$\mathbf{L_1}$	solution	0.475	5.1		6.2
		1:2			1.4	
		1:3			7.5	
	$\mathbf{L_2}$	solution	0.545	7.0		8.0
		1:2			5.2	
		1:3			8.9	
Tb	$\mathbf{L_1}$	solution		34.5		40.0
		1:2			22.2	
		1:3			45.5	
	$\mathbf{L_2}$	solution		36.0		39.4
		1:2			33.6	
		1:3			42.2	

With the assumption that the Ln ions are nine-coordinate, we expect six (1:1), three (1:2), and zero (1:3) water molecules in the first coordination sphere of the metal ions, respectively. Taking the speciation defined above into account, we have checked that the experimental q values are in line with this hypothesis. We indeed calculate $q = 1.4$ for $Eu\mathbf{L_1}$ and $Eu\mathbf{L_2}$, as compared to 1.6 and 1.2 obtained from the lifetime measurements.

The quantum yields of the corresponding solutions in water (Table 6) have been determined with respect to dipicolinate solutions ($Q^{Eu}_L = 13.5\%$, $Q^{Tb}_L = 22.0\%$).[35] They amount to 5.1% ($\mathbf{L_1}$) and 7.0% ($\mathbf{L_2}$) for Eu^{III} while the corresponding data for Tb^{III} are 34.5% ($\mathbf{L_1}$) and 36.0% ($\mathbf{L_2}$). Considering the speciation discussed above, the quantum yields of the 1:3 species must be larger. To assess them, we have measured more concentrated solutions ($[Ln]_t = 8 \times 10^{-5}$ M and $[L]_t = 2.4 \times 10^{-4}$ M, containing 3.5, 16.7, and 79.8% of the 1:1, 1:2, and 1:3 species for $\mathbf{L_1}$ and 2.5, 19.7, and 77.8% for $\mathbf{L_2}$). Under the assumption that contribution from the 1:1 species can be neglected since it would be far less luminescent than the two others, the quantum yields of the 1:3 species can be recalculated and amount to 7.5, 8.9, 45.5, and 42.1% for $Eu\mathbf{L_1}$, $Eu\mathbf{L_2}$, $Tb\mathbf{L_1}$, and $Tb\mathbf{L_2}$, respectively. These values are large, pointing to $\mathbf{L_1}$ and $\mathbf{L_2}$ being good building blocks for the engineering of lanthanide-containing luminescent stains for biomedical analysis.

The total quantum yield Q_{tot}^{Ln} obtained upon ligand excitation can be broken up into three contributions:

$$Q_{tot}^{Ln} = \eta_{ISC}\eta_{ET}Q_{Ln}^{Ln} = \eta_{sens}Q_{Ln}^{Ln} \quad (4)$$

Here η_{ISC} is the efficiency of the intersystem crossing ($^1\pi\pi^* \rightarrow {}^3\pi\pi^*$), η_{ET}, the efficacy of the energy transfer ($^3\pi\pi^* \rightarrow$ Ln), and Q_{Ln}^{Ln}, the intrinsic quantum yield of the lanthanide ion. The latter can be calculated from the observed luminescence lifetime τ_{obs} and the radiative lifetime τ_r, which, in the case of Eu^{III}, can be estimated using eq 6 by assuming that the intensity of the purely magnetic dipole transition $^5D_0 \rightarrow {}^7F_1$ is independent of the chemical environment:[45]

(45) Werts, M. H. V.; Jukes, R. T. F.; Verhoeven, J. W. *Phys. Chem. Chem. Phys.* **2002**, *4*, 1542.

$$Q_{Eu}^{Eu} = \tau_{obs}/\tau_r \quad (5)$$

$$k_r = \frac{1}{\tau_r} = A_{MD,0} n^3 \left(\frac{I_{tot}}{I_{MD}}\right) \quad (6)$$

$A_{MD,0} = 14.65\ s^{-1}$ is the spontaneous emission probability of the $^5D_0 \rightarrow {}^7F_1$ transition, n, the refractive index of the medium, I_{tot}, the ratio of the integrated total emission from the $^5D_0 \rightarrow {}^7F_J$ transitions ($J = 0-6$), and I_{MD}, the integrated emission of magnetic dipole transition $^5D_0 \rightarrow {}^7F_1$. From the experimentally determined ratios for the more diluted solutions, $I_{MD}/I_{tot} = 0.343$ (**L₁**) and 0.258 (**L₂**), we calculate $\tau_r = 9.2$ (**L₁**) and 7.4 ms (**L₂**) and $Q_{Eu}^{Eu} = 5.17\%$ (**L₁**) and 7.35% (**L₂**), which, in turn, leads to η_{sens} values close to 1 (0.98 and 0.95 for **L₁** and **L₂**, respectively), indicating very efficient sensitization processes.

Reinhoudt et al.[46] have shown that the intersystem crossing process becomes effective when $\Delta E(^1\pi\pi^* - {}^3\pi\pi^*)$ is at least 5000 cm^{-1} and empirical rules have been defined for an optimal ligand-to-metal transfer process:[47] for Eu^{III}, $2500 < \Delta E(^3\pi\pi^* - {}^5D_0) < 3500\ cm^{-1}$, and for Tb^{III}, $2500 < \Delta E(^3\pi\pi^* - {}^5D_4) < 4000\ cm^{-1}$. The emission spectra of the complexes with ligands **L₁** and **L₂** are consistent with this finding, since they display an extremely weak emission from both the singlet and triplet states and a strong emission from Eu^{III} and Tb^{III}. It is noteworthy that the metal-centered luminescence is well sensitized, despite the relatively large energy gaps $\Delta E(^3\pi\pi^* - {}^5D_0) \approx 5650\ cm^{-1}$ (**L₁**) and 8000 cm^{-1} (**L₂**) for the Eu^{III} ion; experimentally, however, the quantum yield of the complex with **L₂** is larger than the one with **L₁**. With respect to Tb^{III}, the gap is ideal for **L₁**, $\Delta E(^3\pi\pi^* - {}^5D_4) \approx 2\ 500\ cm^{-1}$, but much larger for **L₂**, 4700 cm^{-1}, although the quantum yield is similar for both compounds. These apparent deviation from the above-mentioned rules of thumb may be explained by a better efficiency of the intersystem crossing process in **L₂** compared with **L₁**, as exemplified by the $\Delta E(^1\pi\pi^* - {}^3\pi\pi^*)$ value for **L₂** (6750 cm^{-1}) closer to the "ideal" 5000 cm^{-1} gap than the corresponding value for **L₁** (7100 cm^{-1}).

Conclusion

We have presented a series of tridentate ligands based on a 5′-methyl-2,2′-bipyridine framework substituted in 6 position by varying coordinating functions. When the latter is a diethyl phosphonic group, as in **L₄**, no (or very weak) interaction occurs with lanthanide cations. Saponification leading to the monoethyl phosphonic ester results in a ligand **L₃** able to weakly coordinate lanthanide cations with formation of intricate mixtures of complexes, possibly of polymeric nature. On the other hand, ligands **L₁** and **L₂**, containing respectively carboxylate and phosphonate functions display much stronger interactions. These ligands are fully deprotonated at physiological pH and form complexes with 1:1, 1:2, and 1:3 Ln/L stoichiometries. The associated conditional stability constants point to a stronger coordination ability of **L₂**, partly due to its dianionic character.

Ligands **L₁** and **L₂** are very good sensitizer of the Eu and Tb luminescence in aqueous solution. This is mainly due to an adequate energy gap between $^1\pi\pi^*$ and $^3\pi\pi^*$ levels, $\Delta E(^1\pi\pi^* - {}^3\pi\pi^*) > 5000\ cm^{-1}$, favoring intersystem crossing. On the other hand, the energy gaps between the ligand-centered $^3\pi\pi^*$ level of **L₁** and **L₂** and the Eu- and Tb-emitting states are substantially larger than the values considered as being optimum for an efficient transfer,[47] especially with **L₂**. Nevertheless, an overall efficient energy transfer is observed and luminescence quantum yields are particularly sizable for the Tb complexes.

The anionic tridentate units of **L₁** and **L₂** form stable, water-soluble, and highly luminescent complexes with Eu an Tb and appear as very attractive synthons for the development of more elaborate architectures and for their use in time-resolved applications such as fluoroimmunoassays,[4] luminescence microscopy,[48] or luminescent resonant energy transfer experiments.[49] The use of such platforms provides an easy entry into novel negatively charged multitopic ligands bearing adequate functionality to behave as efficient labels.

Acknowledgment. This work is supported by the French CNRS and by the Swiss National Science Foundation. We thank Frédéric Gumy for his help in recording the luminescence data.

Supporting Information Available: A table listing the energy of the absorption and emission bands of the ligand in water, experimental and calculated UV−vis spectra during the titration of ligands **L₁**−**L₃** in water, ^1H and ^{31}P NMR spectra during the titration of **L₁**−**L₃** in D_2O, speciation in the Eu/**L₁** and Eu/**L₂** systems, and fluorescence and phosphorescence spectra at 295 and 77 K of **L₁**, **L₃**, and **L₄** and of their Ln complexes. This material is available free of charge via the Internet at http://pubs.acs.org.

IC049118X

(46) Steemers, F. J.; Verboom, W.; Reinhoudt, D. N.; van der Tol, E. B.; Verhoeven, J. W. *J. Am. Chem. Soc.* **1995**, *117*, 9408.
(47) Latva, M.; Takalo, H.; Mukkala, V.-M.; Matachescu, C.; Rodriguez-Ubis, J. C.; Kankare, J. *J. Lumin.* **1997**, *75*, 149.
(48) Marriott, G.; Clegg, R. M.; Arndt-Jovin, D. J.; Jovin, T. M. *Biophys. J.* **1991**, *60*, 1374.
(49) Bazin, H.; Préaudat, M.; Trinquet, E.; Mathis, G. *Spectrochim. Acta A* **2001**, *57*, 2197.